

THE HERSCHEL COLD DEBRIS DISKS: CONFUSION WITH THE EXTRAGALACTIC BACKGROUND AT 160 μm

ANDRÁS GÁSPÁR AND GEORGE H. RIEKE
Steward Observatory, University of Arizona, Tucson, AZ, 85721

June 28, 2018

ABSTRACT

The Herschel “DUST around NEArby Stars (DUNES)” survey has found a number of debris disk candidates that are apparently very cold, with temperatures near 22K. It has proven difficult to fit their spectral energy distributions with conventional models for debris disks. Given this issue we carefully examine the alternative explanation, that the detections arise from confusion with IR cirrus and/or background galaxies that are not physically associated with the foreground stars. We find that such an explanation is consistent with all of these detections.

Keywords: circumstellar matter – planetary systems – infrared: stars

1. INTRODUCTION

Debris disks play a vital role in our understanding of the exterior parts of planetary systems. While inner orbit (< 5 AU) planets are now readily observed with various techniques (i.e., radial velocity and planetary transit surveys), wider orbit planets are significantly more difficult to detect, with only a handful of them discovered by direct imaging (Marois et al. 2008; Kalas et al. 2008; Lagrange et al. 2010; Rameau et al. 2013; Currie et al. 2014; Kraus et al. 2014; Bailey et al. 2014). However, with their large surface areas, even low mass and low density debris disks are relatively easy to detect in the mid- to far-infrared wavelengths at larger stellocentric distances, providing ways to study the outer parts of the systems.

Debris disks have a number of characteristic temperatures, of which the most prominent are 190 K (Morales et al. 2011) and 45 – 80 K, with a weak dependence on the spectral type of the star (e.g., Ballering et al. 2013). Our solar system is an example, with the Asteroid belt at 2.3–3.3 AU and Kuiper belt at 30–50 AU (Backman et al. 1995; Vitense et al. 2012).

An intriguing new result from *Herschel* was the discovery of a new class of cold debris disks (Eiroa et al. 2011, 2013), with characteristic temperatures of 22 K. Scaling from the models for Kuiper Belt dust by Yamamoto & Mukai (1998), such a disk would be located at about 120 AU, in an environment dramatically different from those normally assumed for debris disks. The properties of such disks have been studied by Krivov et al. (2013), who concluded that they would need to be made up of particles that are larger than a few millimeters and smaller than 10 km, that are dynamically quiescent, and have orbital eccentricities and inclinations ≤ 0.01 . Systems with such specific parameters are not just difficult to form, but also challenging to maintain, when one considers all the destructive external effects disks at large stellocentric regions (especially ones outside the “stello-pause”) may experience (e.g., erosion by the interstellar medium, stellar fly-bys, etc.).

In this paper, because of the issues detailed above, we re-evaluate the possibility that these excesses are not intrinsic to the stars but result from confusion with unrelated sources. In section 2, we show that both likely forms of confusion noise, IR cirrus and distant background galaxies, would match the apparent temperature of the cold excesses. In section 3, we

show that standard treatments of confusion noise suggest that such sources may significantly affect the apparent detection of cold debris disks. In section 4, we follow up this possibility with a Monte Carlo analysis, which we then use in section 5 to evaluate the null hypothesis that the apparent cold disks are instead drawn from the populations of confusing sources. In section 6, we investigate the dependence of the results on the interval of the background galaxy fluxes considered in the statistical analysis, while in section 7, we compare our results to previous statistical analyses. Finally, in section 8, we summarize our results.

2. POSSIBLE SOURCES OF FALSE COLD DISK SIGNATURES

The cold debris disks have a characteristic temperature of 22 K (Eiroa et al. 2011). At this temperature an excess by a factor of two at 160 μm yields an excess by only a factor of 1.2 at 100 μm . That is, an excess below typical detection limits at 100 μm and shorter wavelengths can be substantially above the stellar output at 160 μm . We now consider whether the SEDs of the possible confusing sources are consistent with this value.

First, we consider confusion by infrared cirrus. There are a number of relevant measurements: 1.) Roy et al. (2010) use BLAST data to find temperatures of 19.9 ± 1.3 K and 16.9 ± 0.7 K for cold interstellar dust in two regions; 2.) Martin et al. (2010) fit early Herschel data with a temperature of 23.6 ± 1.0 K; 3.) Bracco et al. (2011) find $T = 19.0 \pm 2.4$ K, using a different set of early Herschel data; 4.) Veneziani et al. (2013) use Bayesian methods with a broad set of data to find temperatures in the ISM cold dust of ~ 20 K with a range of about 4 K around this value. Therefore, IR cirrus is a viable candidate to contribute to emission at the appropriate temperature for the apparent cold disks.

We now turn to confusion by background galaxies. There are a number of systematic changes in the SEDs of luminous galaxies with increasing redshift (and increasing luminosity at the detection threshold (e.g., Rujopakarn et al. 2013; Berta et al. 2013; Symeonidis et al. 2013, and references therein)). We have quantified these trends as in Rujopakarn et al. (2013). We have fitted a blackbody to the appropriate galaxy SED for direct comparison with the assumed disk SED in Eiroa et al. (2011). We take luminosities between the lower envelope of the distribution of detection limits with redshift in Magnelli et al. (2013, Figure 8)

and twice this value, to obtain luminosities as a function of redshift, characteristic of the faintest sources detected with PACS. We then redshift blackbody fits to the SEDs for the appropriate luminosities by the appropriate values to obtain apparent temperatures of faint $160\ \mu\text{m}$ detections vs. redshift. We find that the values range from about 25 K at $z = 0.4$ to about 29 K near $z = 0.8$, from where they decline to about 20 K at $z = 2$. Magnelli et al. (2013) give redshifts of $z = 1.22^{+0.68}_{-0.41}$ and $z = 0.94^{+0.52}_{-0.38}$ (interquartile ranges) respectively for $160\ \mu\text{m}$ sources fainter and brighter than 2.5 mJy. Thus, the faint detections should fall within the 20 - 29 K apparent temperature range. The temperatures estimated from the 100 and $160\ \mu\text{m}$ measurements of the six sources identified as having cold excesses in Eiroa et al. (2013) range from 22.5 to 31 K for the three with probable weak $100\ \mu\text{m}$ excesses (HIP 73100, 92043, and 109378) and from $2\ \sigma$ upper limits of 21 to 26.5 K for the three with no indicated $100\ \mu\text{m}$ excesses (HIP 171, 29271, and 49908). We conclude that the expected spectral behavior of faint background galaxies is consistent with the temperatures assigned to the cold debris disks.

3. ESTIMATES OF THE EFFECTS OF CONFUSION NOISE

Confusion with distant background galaxies becomes an increasing issue with increasing wavelength for the Herschel instruments. A conventional definition of the confusion limit is the ‘‘source density criterion (SDC)’’, when 10% of the sources of a given flux are so tightly crowded that they cannot be measured. Dole et al. (2003) find that this limit corresponds to 16.7 beams per source, where the definition of the beam area is based on that by Condon (1974). Berta et al. (2011) estimate that the SDC is reached for Herschel at source flux densities of 0.4, 1.5-2, and 8 mJy respectively at 70, 100, and $160\ \mu\text{m}$. Given the fall of a stellar photospheric output inversely as the square of the wavelength, the SDC is a significant issue for the Eiroa et al. (2013) sample only at the longest wavelength band of these three. However, the flux densities attributed to the cold disks are very similar to the limit there. Of the ~ 100 sources without $100\ \mu\text{m}$ excesses, the confusion statistic would imply that roughly 6 would be confused with background galaxies at 8 mJy or brighter, compared with the six sources identified by Eiroa et al. (2013) as cold disk sources, some of which have excess fluxes less than 8 mJy. This agreement calls for a more detailed investigation.

Hogg & Turner (1998) show that sources near the confusion limit and with low ratios of signal to noise tend to be biased too high in apparent brightness. They derive a correction dependent on the slope of the source counts and the signal to noise ratio of the source, to remove this bias and assign the maximum likelihood flux to a source. In the case of the $160\ \mu\text{m}$ galaxy measurements, a slope of $q = 0.9$ can be derived for the source counts from the Magnelli et al. (2013) data between 1 and 10 mJy, while the signal to noise ratios can be obtained from Eiroa et al. (2013), Table 14. Table 1 shows the six cold disk candidate stars with the resulting estimates of the fluxes from the disks alone at $160\ \mu\text{m}$. We have left the error estimates as in Eiroa et al. (2013), although Hogg & Turner (1998) argue that the errors should be expected to increase in these nearly-confusion-limited cases (see their Figure 2 and also Figure 3 in Hogg 2001). Four of the six candidates have dropped below the usual $\chi_{160} > 3$ detection criterion¹, suggesting that a more detailed treatment of

¹ $\chi_{160} = (F_{160} - P_{160}) / \sigma_{160}$, where F is the measured flux, P is the estimated photosphere, and σ is the error of photometry.

Table 1
Parameters of the Monte Carlo analysis.

Variable	Description	Fiducial value
D	Size of artificial field	0.5 sq. deg.
G_{\min}	Minimum galaxy flux considered	1 mJy
G_{\max}	Maximum galaxy flux considered	225.42 mJy
b_{gal}	log bin size in the galaxy distribution	0.02
σ_{cirrus}	Std. dev. of cirrus noise	0.505 mJy
μ_{limit}	Location par. of noise log-norm distr.	0.67
σ_{limit}	Scale par. of noise log-norm distr.	0.33
N_*	Number of positions tested	10^6
r_t	Target radius	6''
r_p	Photometry radius	8''
S_{in}	Sky aperture inner radius	18''
S_{out}	Sky aperture outer radius	28''
ΔB_*	Bin size in photometry distribution	0.1 mJy

the confusion effects may be critical in evaluating the reality of the cold disks.

4. MONTE CARLO ANALYSES

The preceding sections indicate that confusion noise may play a significant role in mimicking the signature of a hypothetical extremely cold debris disk. We therefore perform various Monte Carlo analyses, allowing a relatively easy exploration of the confusion noise in more detail within the full parameter space. Our analyses considers two main sources of obtained flux: cirrus noise and background galaxies. We detail these in the following subsections, while in Table 1 we summarize the parameters of the analyses with the default values given. The numerical variables of the model (i.e. the size of the artificial field, log bin size in the galaxy distribution, Airy pattern bin size) were determined with convergence tests to ensure fast computational speeds with reliable results.

4.1. Cirrus noise

Determining the value of the cirrus noise is difficult. Because of this, our goal was to assign a highly conservative value to it, without neglecting it. This was also appropriate, as the DUNES survey was designed to observe sources in low cirrus background regions. We used Equation 22 of Miville-Deschênes et al. (2007) to calculate the confusion noise, which is based on the power-spectrum of the far-infrared dust emission and calibrated to low levels. The spectral index in the equation is given by Equation 4 in their paper. Using HSpot, we estimated the average ISM flux background for the DUNES sources to be $\langle I_{160} \rangle = 7.02\ \text{MJy sr}^{-1}$, and a $\langle I_{160} \rangle / \langle I_{100} \rangle$ ratio of 1.845. Assuming the standard Condon (1974) definition of beam size, we derived a cirrus noise of $\sigma_{\text{cirrus}} = 0.505\ \text{mJy}$. This estimate is only about half as large as is indicated in the scaling relations in HSpot. We dealt with the small number of sources with much stronger than average cirrus by eliminating them from our test sample, rather than trying to estimate the cirrus noise more accurately. In the Monte Carlo simulations the cirrus noise value at each test location was determined by choosing a value following a Gaussian probability function centered at zero with a standard deviation of σ_{cirrus} .

4.2. Background galaxy contribution

As introduced in section 3, background galaxies can dominate the confusion noise at far-IR wavelengths. For our Monte Carlo analyses, we randomly distributed galaxies on a 0.5 sq. degree area, with a fiducial galaxy flux interval

Table 2
The number of cold disk sources observed and predicted at various target radii.

	Observed	Data Realization		CDF	
		Point-source [†]	PSF Smoothed [†]	Point-source	PSF-smoothed
6'' Target Radius	6	6.7	6.4	6.1	5.6
7'' Target Radius	6	8.6	7.4	7.9	6.5
8'' Target Radius	7	10.6	8.3	9.9	7.3

[†] Number of sources predicted at the location of the peak of the probability distribution in the data realization analysis (section 5.2).

of 1 to 225 mJy, although for certain tests we extended the lower limit to 0.012 mJy. The galaxy number counts were adopted from three separate studies. Between 0.012 and 1.25 mJy we used the modeling results found in Table B.2 of Franceschini et al. (2010), between 1.42 and 28.38 mJy we adopted the observed galaxy counts of the GOODS-S ultra-deep Herschel survey from Magnelli et al. (2013), while the number counts of the brightest galaxies were adopted from Table 5 of Berta et al. (2011) (all fields combined). Although these are three independent studies, their differential number count curves connect smoothly. Total number counts were calculated in logarithmically evenly spaced flux bins, with the number counts appropriately interpolated (in log space) at the bin boundaries and integrated (also in log space) with a simple second order trapezoid method. Between 1 and 225 mJy the artificial field (0.5 sq. degree) has altogether 19146 galaxies, and between 6 and 13 mJy it has ~ 2776 galaxies (or ~ 5552 galaxies per sq. degree), which agrees with the estimated 5500 galaxies per sq. degree in this interval cited by Krivov et al. (2013).

When considering confusion with background galaxies, Eiroa et al. (2013) only used the differential count value determined at 6 mJy, resulting in a smaller total number of estimated background sources (~ 2000 per sq. degree). As detailed in section 6, one of the key differences between our analyses and the previous ones is that we use a larger interval of background galaxy fluxes (and integrate the differential distribution). As we will show, galaxies fainter than the detection threshold (≤ 6 mJy) contribute to the confusion noise, as their spatial distribution is not isotropic enough for their contribution to the total flux to be canceled out by sky subtraction, even when considering a completely random field as we do here. Natural clustering of galaxies will likely even enhance their contributions (Fernandez-Conde et al. 2008).

The results of our model will depend predominantly only on a single parameter, the beam solid angle (Ω) (i.e., the confusion beam size). The value of the beam solid angle is a matter of definition. The classic Condon (1974) definition of the effective beam solid angle is

$$\Omega_e = \left(\frac{1}{4}\pi\Theta_1\Theta_2\right) \frac{1}{(\gamma-1)\ln 2}, \quad (1)$$

where Θ_1 and Θ_2 are the half-power axes of the elliptical Gaussian beam and γ is the slope of the differential distribution of sources. According to Table 3.1 of the PACS Observer’s Manual, $\Theta_1 = 10.65''$ and $\Theta_2 = 12.13''$ at a scan speed of $20'' \text{ s}^{-1}$, while the value of γ is around 1.9 at low fluxes (1 - 10 mJy), according to the Magnelli et al. (2013) data. These yield an effective beam solid angle of $162''^2$, or a confusion beam radius of $7.19''$.

The DUNES team uses the images to identify potentially confusing sources (of similar brightness to the target) at $\geq 6''$.

Hereafter, we refer to this distance as the *target radius*. After excluding targets with confusing sources, they perform photometry in a photometry radius of $8''$. The sky background was subtracted based on a value measured in an annulus outside the photometry radius. Our models were constructed to reproduce this measurement strategy. We assumed aperture photometry carried out within a radius of $8''$. We tested a variety of target radii inward of which we assumed it was no longer possible to distinguish a background source from the target, besides the $6''$ assumed by DUNES. In all models, we rejected targets with sources lying in the annulus between the target and photometry radii that also were more than 2.5σ above a value chosen with a log-norm probability function with μ_{limit} and σ_{limit} parameters (see Table 1) that describes the distribution of photometry errors for the DUNES sample.

We integrate the flux of the sources within the photometry aperture and the corresponding sky annulus using two methods: treating the galaxies as point sources in one of them, and convolving their emissions with the Herschel Airy pattern at $160 \mu\text{m}$ in the other. The first is the traditionally used method when considering confusion, however, we have found that smoothing the emissions with the point spread functions (PSF) will affect the results of the confusion estimates. We introduce the results of both calculations for completeness and also to allow comparisons with previous work.

After generating the artificial background galaxy map, our code determined random positions and performed the previously described ‘‘aperture photometry’’. For the smoothed model all partial fluxes contained within the apertures were included (i.e., fluxes from sources both within and outside the apertures). For the point source method the total fluxes of sources within the apertures were added to determine the total flux, but only for sources that were located within the apertures. To censor bright galaxies within the sky annuli, as was done by Eiroa et al. (2013), we removed bright galaxies from the sky annulus above a simulated upper limit. As with the photometry aperture, this limit was set at $2.5 \times a \sigma$ value that was randomly chosen from the photometry error distribution described above. Finally, the flux within the sky background was normalized by the ratio of the aperture area to the sky annulus area. The flux at the test location was then determined by subtracting the ‘‘sky background’’ from the flux determined within the confusion beam aperture and adding the cirrus noise.

5. STATISTICS

In this section, we compare the results of our model to the DUNES observations. We first define the DUNES sample we compare our models to, and then compare the model results to the observations with various statistical methods, while varying the target radius. In Table 2, we summarize the detection statistics of the observations and the models.

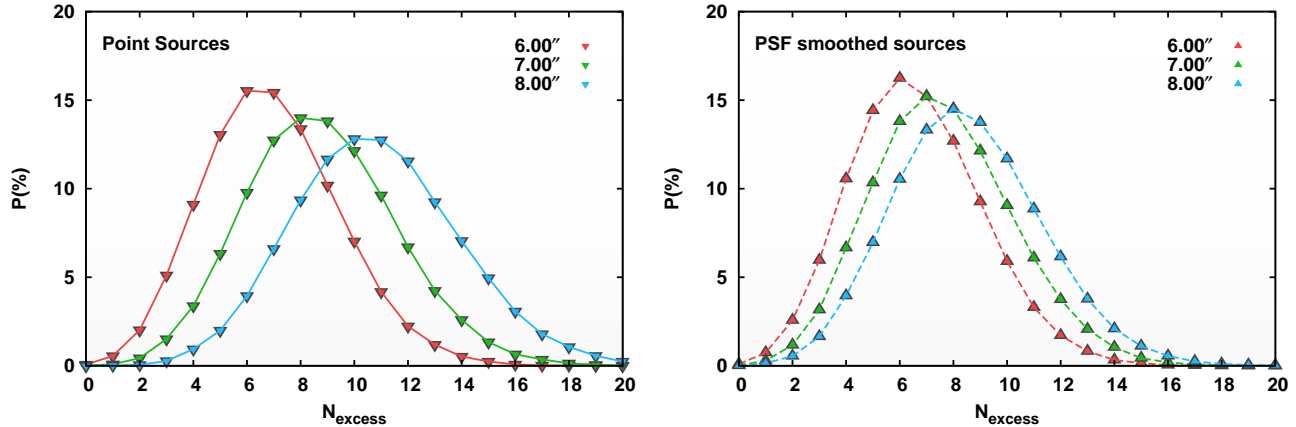


Figure 1. The probabilities of detecting certain number of cold sources at various target radii, using the data realization method described in section 5.2. In the *left panel*, we show the results of the “point sources” model and in the *right panel*, we show the results of the “PSF smoothed sources” model.

Table 3
Maximum Likelihood 160 μm Flux Density Estimates

Star HIP	Max. Likelihood 160 μm disk flux density (mJy)	Error (mJy)	χ_{160}
171	6.2	2.5	2.5
29271	6.0	2.2	2.7
49908	4.8	2	2.4
73100	8.3	2.5	3.3
92043	9.3	4	2.3
109378	9.8	2	4.9

5.1. The DUNES sample

There are 133 sources in the DUNES sample (Eiroa et al. 2013) of which 131 have data at 160 μm . Of these, 100 sources do not have detectable excesses at either PACS wavelengths. From these 100, we removed 6 sources whose limits on their 160 μm excess were higher than the typical value within the sample (HIP 71681, HIP 71683, HIP 88601, HIP 104214, HIP 104217, and HIP 108870). Of the remaining 31 excess sources, Eiroa et al. (2013) list 6 as harboring cold debris disks. Although it is listed as a cold disk candidate, the excess for HIP 92043 is detected at 70 μm (both MIPS and PACS) and at 100 μm and 160 μm (Eiroa et al. 2013), so its identification as a cold disk candidate depends on the relatively weak 160 μm result in Table 1. We computed a weighted average of the MIPS and PACS 70 μm data, obtaining an excess of 11.9 ± 3.3 mJy, took the 100 μm result from Eiroa et al. (2013) and the maximum likelihood value at 160 μm from Table 3 and then fitted the excess spectral energy distribution at all three wavelengths with a modified blackbody with $\beta = 0.65$ (Gáspár et al. 2012). We found that a disk temperature of 62 K fitted within the errors ($\chi_{\text{reduced}}^2 = 1.35$), so there is no need to hypothesize a cold disk for this star and we remove it from the cold disk sample. Of the original 6 cold debris disk candidates (Eiroa et al. 2013), we only consider HIP 171, HIP 29271, and HIP 49908 most likely to have alternative explanations for their apparent far infrared excesses. HIP 73100 and HIP 109378 show evidence for excess emission at 100 μm , but the rapid increase in their SEDs to 160 μm probably arises from confusion.

Apart from the five cold disk candidates, additional spurious sources were listed in Table D.1 of Eiroa et al. (2013). Two of the spurious sources have heavy cirrus contamina-

tion [HIP 29568 (“structured background”) and HIP 71908 (“emission strip”); HSpot indicates a high interstellar background level of 59.7 MJy sr^{-1}] and one is probably a spurious detection (HIP 38784). Four of the remaining sources (HIP 40843, 85295, 105312, and 113576) are potentially contaminated by background galaxies. Of these four sources, two have the peaks of the emission of their 160 μm component within the 8’’ photometry aperture of the survey (HIP 85295 at 4.8’’ and HIP 105312 at 7.16’’). For our models to stay consistent with the observational sample, we include these two sources in the cold disk sample (one or two of them, depending on the size of the target radius). This means that there are a total of six/seven sources with apparent cold excesses (HIP 171, HIP 29271, HIP 49908, HIP 73100, HIP 85295, HIP 105312, and HIP 109378).

This leaves us a total sample of 93/94 sources (6/7 with excess and 87 without), depending on the considered target radius, with the boundary at 7.16’’. Of the non-excess sources, 33 have measured fluxes, while the remaining 54 only have upper limits. The remaining 25 sources with detected debris disk excesses were not included in the statistical analysis, as estimating a possible level of contamination for them is not possible. Of these sources, three (HIP 4148, HIP 27887, and HIP 51502) have equilibrium temperatures around 30 K, close to the levels of the cold disk candidates. The final results of the paper would indicate an additional 1.98 cold sources remaining in the sample of 25, possibly also explaining the far-IR excesses observed at these three sources.

5.2. Method 1: Via Realization of Data

The first method we apply realizes artificial datasets and counts the number of detections within the dataset. First, 93/94 source locations are randomly selected within our artificial field and the total flux at these locations calculated according to the procedure described in section 4. Then a detection threshold (determined at $3\sigma_F$) is randomly paired to each artificial location from the sample of 93/94 DUNES sources. If the total flux is larger than the detection threshold then the number of detections in the realized dataset is incremented by one. We realized 10^5 datasets of 93/94 sources for each of the tested target radii. In Figure 1, we show the results of these tests for both the “point sources” and “PSF smoothed sources” models and in Table 2, we summarize the detection statistics of the model. The probability of finding

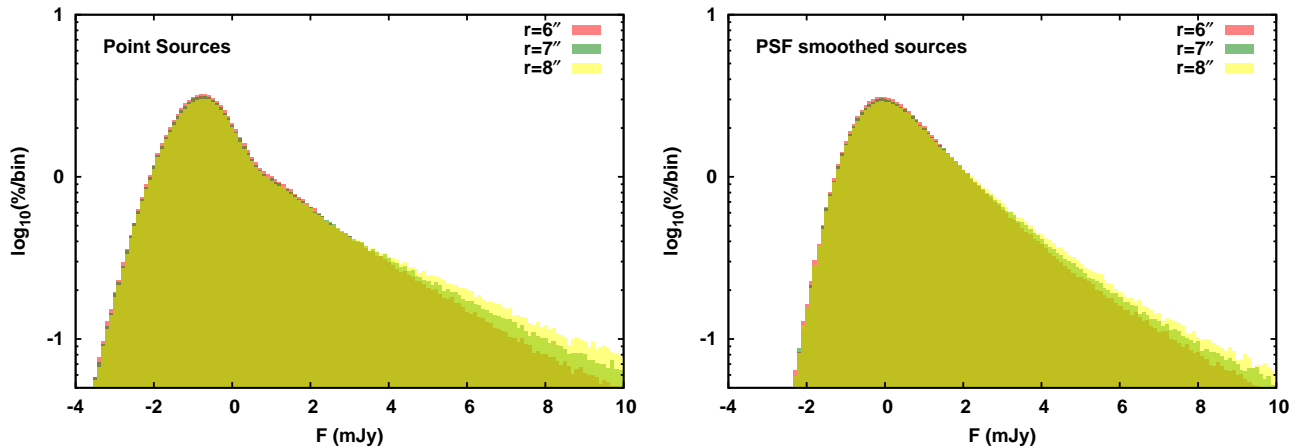


Figure 2. The distributions of background fluxes assuming the fiducial values of the model, varying only the confusion beam radius. In the *left panel*, we show the results of the “point sources” model and in the *right panel*, we show the results of the “PSF smoothed sources” model.

more sources increases with larger target radii, as expected.

The “point-sources model” yields probability curves that are strongly dependent on the target radii. With over 40% of the photometry area located between 6 and 8”, sensing confusing sources in the outer aperture is critical. The probability curves are wide, for example at a target radius of 7”, the model predicts 8.55 ± 2.79 sources, meaning that detecting 5.7 sources is just as likely as detecting 11.3.

A closer representation of the measurements is performed by the “PSF smoothed-sources model”. The distributions are narrower and the peaks are closer and at lower values than for the simpler “point-sources model”. The peaks shifting to lower values is due to the generally higher sky background values, which is a result of contributions to the sky flux from sources outside the reference sky annulus, which are now smoothed into the sky area. As the sky annulus is larger in area than the aperture photometry area, and it also receives contributions from sources inside of it as well as from outside of it, this is a significant effect. Moreover, the distributions are also narrower due the PSF smoothing, as background levels become more homogenous. As an example, at a target radius of 7”, the “PSF smoothed-sources” model predicts 7.38 ± 2.61 sources. This agrees well with the 6/7 sources expected at 7.16” according to the observations.

The significant number of potentially confusing sources among the stars without excesses or with cold ones raises a question of the contamination among those with debris disks. A rough estimate can be obtained by noting that among the stars with normal disks, there are five with apparent detections at $160 \mu\text{m}$ ($\chi_{160} > 3$) and with flux densities less than 20 mJy, within the range where confusion is a risk. From the statistics above, these numbers suggest that no more than one of the normal disk stars may have a $160 \mu\text{m}$ flux density dominated by a background galaxy.

5.3. Method 2: Via Distribution Functions

With the second method, we generated distributions of the artificial fluxes by testing N_* number of random positions. The flux values of our sample of N_* test points were then binned with a bin size of $\Delta B_* = 0.1$ mJy. These distributions were then compared to the observed distribution of fluxes with various methods.

5.3.1. Percentages with Cumulative Distributions

The simplest test that can be performed is determining the percent of sources above given thresholds using the cumulative distribution function (CDF) of the model (as in Krivov et al. 2013; Eiroa et al. 2013). This test is not rigorous (e.g., it does not take account of upper limits above the sample detection threshold). However, for illustration and to allow comparison with previous statistical analysis, we begin with the results of this test. In Figure 2, we show binned distribution functions of background fluxes of our nominal model, while varying the target radius, for both the “point sources” and “PSF smoothed sources” models. Increasing the target radius, as expected, will widen the distribution and yield more high flux sources. The faintest cold disk candidate has an excess of 6.39 mJy. The number of predicted sources above this limit at various target radii is also summarized in Table 2. The results of the CDF analysis compare fairly well to the observed number of sources with cold disk signatures, especially when considering the classic Condon (1974) definition of confusion beam size and the more realistic “PSF smoothed sources” model.

The peak of the distribution at negative values in Figure 2 results because more brighter galaxies will be located within the larger area sky annulus than within the search area. Unless the area of the sky annulus is equal to the photometry aperture area, this will always result in a negative bias. We have tested this by using a sky annulus with the same area as the photometry aperture, resulting in a peak at zero. The effect is less prominent in the “PSF smoothed sources” model compared with the “point sources model”.

5.3.2. Kaplan-Meier estimates

The Kaplan-Meier (KM) estimates (Kaplan & Meier 1958) of both the modeled and observed distributions provide a systematic method to compare these distributions while taking account of the upper limits (or censoring) in the observations. The KM method has been adopted for astronomical data analysis (e.g., Feigelson & Nelson 1985), where it is useful for randomly picked datasets, such as the background distribution in the DUNES survey. We used the ASURV package (Feigelson & Nelson 1985) to calculate the KM estimates and compare the KM curves of the observations and models at various target radii in Figure 3. The DUNES data we compare our models to depends on the target radius with the addition of the extra seventh source when comparing to the 8”

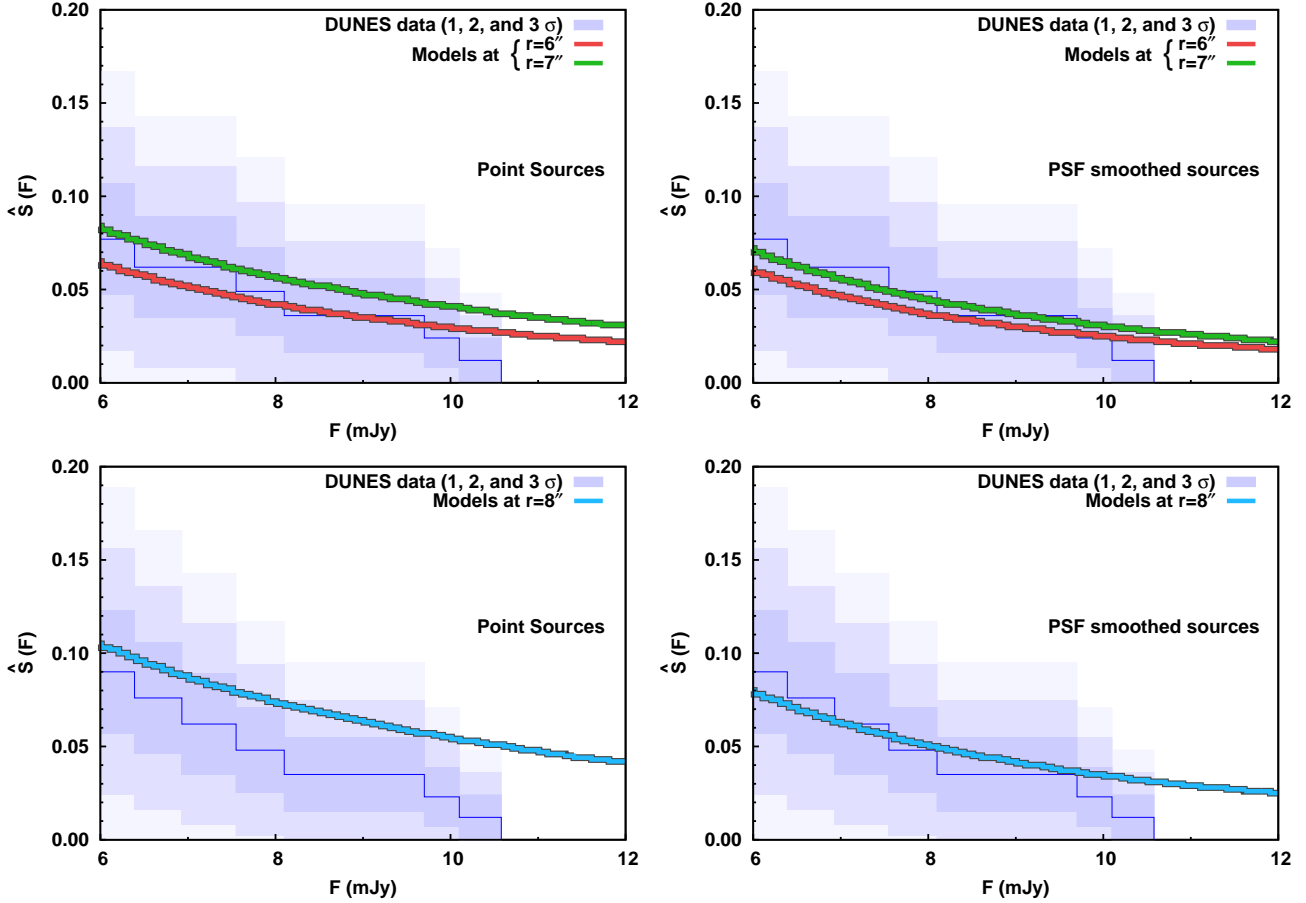


Figure 3. The KM estimates (see section 5.3.2) of the observation and the models. The blue histograms show the 1, 2, and 3 σ confidences of the KM estimates for the observations. The 8'' models (*bottom panels*) are compared to the 94 source DUNES sample, while the 6 and 7'' models (*top panels*) are compared to the 93 source DUNES sample.

model. The bottom panels in the Figure show these calculations, while the top panels show the comparisons at 6 and 7'' with the KM curve of the observations using six excess sources. For the observations, we have set all sources apart from the cold disk candidates (the remaining 87 sources) as upper limits. The upper limits were set to $UL = F - P + 3\sigma_F$ for sources where the photospheres were detected and kept at their original published upper limit value minus the estimated photosphere where they were not. Here, F is the measured flux density, P is the expected value from the stellar photosphere, and σ_F is the quoted uncertainty. The models generally appear to agree closely with the distribution of the observations.

5.3.3. Kolmogorov-Smirnov test on the incompleteness-corrected sample

There is no standard method to determine the probability of agreement between censored data and a numerical model. We have therefore proceeded as follows. The Kaplan-Meier estimator introduced in the previous subsection can be thought of as an incompleteness-corrected CDF, as it carries on the probabilities of previous events occurring with the knowledge of the censoring. To obtain a rigorous test making use of the upper limits, we perform a Kolmogorov-Smirnov (KS) test on the incompleteness-corrected sample, by increasing the weight of the surviving sample members exactly the way an incompleteness correction would. The KS statistic was

only calculated for sources above the detection threshold of 6.39 mJy (as below we do not have any data) and the probabilities were calculated by scaling with the complete distribution. In Figure 4, we show the probabilities obtained as a function of the target radius with these methods. The probability curve indicates that the data are consistent with being drawn from the confusion-limited model at $> 80\%$ confidence for all target radii between 2 and 8'' (the drop in probability for large radii is because the model predicts too many detections, so this case is not of interest). This range of target radii includes all plausible definitions for the PACS beam. The figure shows that even when considering a smaller target radius, as long as the photometry is performed up to 8'', the model results will be consistent with the observational statistics.

We also performed the Anderson-Darling K-sample test (Scholz & Stephens 1987) on the incompleteness corrected sample, as it is more sensitive at the edges of the distributions than the KS test, using the statistical analysis software package R. The observed data has many upper limits above the detection threshold of 6.39 mJy, and hence has significant corrections for incompleteness. These corrections introduce pseudo-ties in the data, to which the Anderson-Darling test is sensitive. Therefore, we used the method that assumes ties within the data, described in section 5 of their paper. The analysis showed that the two distributions are indistinguishable within target radii of 4.2 and 6.3'' for the ‘‘point sources’’ model and for all target radii larger than 5.3'' for the ‘‘PSF

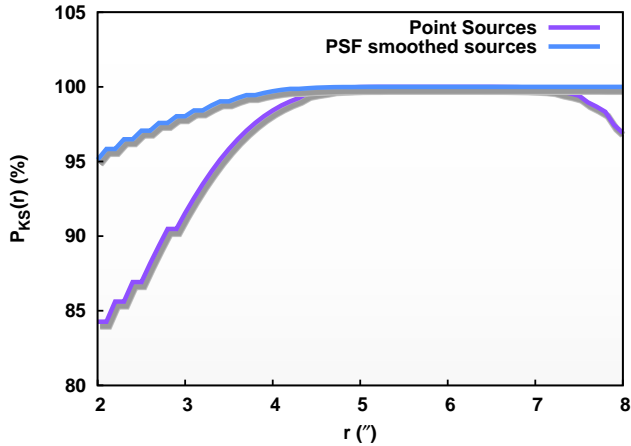


Figure 4. Probability of agreement between the incompleteness corrected data and the model as a function of the confusion beam radius.

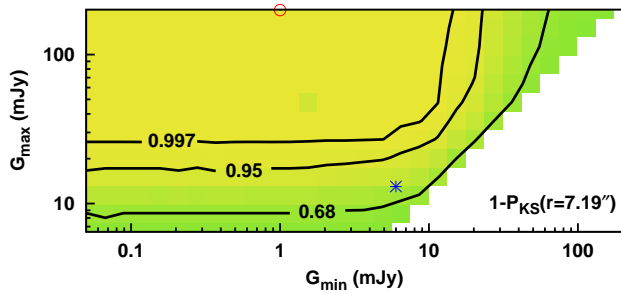


Figure 5. The probability of agreement between the incompleteness corrected data and the model as a function of the minimum and maximum galaxy fluxes considered in the model. The blue star shows the interval considered by Eiroa et al. (2013) and Krivov et al. (2013) and the red circle shows the interval considered by our nominal model.

smoothed sources” model at a 95% confidence level.

6. PARAMETER DEPENDENCE

Although the results mainly depend on the choice of target radius, here we investigate how the results depend on the range of galaxy fluxes considered. The main motivations for this study are the previous analyses (Eiroa et al. 2013; Krivov et al. 2013) that rejected the hypothesis that all of these systems could be explained by confusion, but only used a limited range of galaxy fluxes, between 6 and 13 mJy.

We simulated 900 models, with both the minimum and maximum galaxy fluxes ranging between 0.012 and 225.49 mJy and a target radius of 7.19” using the PSF smoothed approach, and calculated the completeness corrected KS test (as in section 5.3.3) for each of them. In Figure 5, we show the results of these KS tests as a 2D plot, contouring the 1, 2, and 3 σ probabilities and also plotting the ranges considered by the previous studies and ours. Compared with the full-range estimate, the limited flux interval produces less sources through the omission of noise due to the cumulative effects of faint sources. This result demonstrates that the difference between our work and the previous conclusions about the cold disks can largely be explained by the inappropriate limitation in confusing source fluxes assumed by Eiroa et al. (2013) and Krivov et al. (2013).

7. COMPARISON TO PREVIOUS WORK

The DUNES and DEBRIS Herschel Open Time Key Program surveys were the first surveys ever conducted with the specific goals of detecting debris disks at wavelengths between 100 and 800 μm . At these wavelengths, as shown in Section 2, confusion with the extragalactic background and/or infrared cirrus can be an important effect. While simple galactic number count statistics suffices for confusion studies at shorter wavelengths, due to the larger confusion beam sizes and the high number of confusing sources at the detection threshold, a more sophisticated analysis is necessary at these longer wavelengths.

In the discovery paper, Eiroa et al. (2013) analyze the likelihood of these sources originating from confusion with the extragalactic background in their Section 7.2.1. After excluding spurious sources with obvious high background/cirrus contamination, they conclude with a list of six sources requiring an alternate explanation. Based on the Berta et al. (2011) galaxy counts at 160 μm , they perform count statistics. Based on their artificial data tests, they assume a confusion beam radius of 5”, where they were able to separate two equal sources with fluxes near the detection threshold value. For multiple sources that are fainter than the detection threshold, this may be an inadequate confusion beam radius value, especially when considering the classic Condon (1974) definition of confusion beam size. They also use the differential number density of galaxies at the detection threshold as a total source count, yielding a low number of possible contaminating sources. In Section 6, we show the importance of using the full range of background galaxy fluxes when calculating the effects of confusion. Finally, they considered their complete observational catalog for the statistics (133 sources), including systems that were shown to harbor debris disks. Although systems with debris disks may also have background confusion at 160 μm , the contribution from the background will be difficult to distinguish from the debris disk component, requiring these systems to be removed from the analysis sample. These approximations resulted in a prediction of only 1.2% of the sources having background confusion.

The theoretical analysis in Krivov et al. (2013) focused on explaining the physical likelihood of cold debris disks existing and deem it unlikely that all of these sources could originate from confusion with cirrus, which we agree with. They performed searches for strong X-ray and/or optical galactic counterparts, but the results from these tests were largely inconclusive within the confusion beam. As in Eiroa et al. (2013), they also performed statistical tests, mostly with the same arguments. They show that the offsets between the assumed position of the sources and the 160 μm fluxes are all within 5”, however, as per the definition of confusion beam (7.19”), all positions within it are not separable. This is also noted in Krivov et al. (2013), which is why they search for sources of background confusion within a radius of 6” in their statistical analysis. However, they only look at extragalactic sources within the flux range of the cold sources (6 to 13 mJy), not accounting for possible confusion originating from multiple fainter sources. They calculate a confusion probability of 4.8%, and scaling to the complete DUNES sample (133 sources) predict 6.4 false detections. Assuming that all of the seven spurious sources in Table D.1 of Eiroa et al. (2013) are a result of extragalactic background contamination, they determine that there is a 69% probability that the remaining six cold disks are true debris detections. This argument, however,

does not take into account that two of the seven sources are obviously contaminated by high cirrus noise (HIP 29568 and HIP 71908), while three of the remaining five (HIP 40843, HIP 105312, and HIP 113576) have the peaks of their 160 μm emission outside of the 6'' confusion beam radius used in their analysis. Of the remaining two sources, HIP 38784 is a spurious detection with double 160 μm peaks (of which one is also outside of the 6'' radius). There is only a single source from their Table D.1, HIP 85295, that needs to be counted as a source in the statistical analysis, as in our paper.

The most detailed work on confusion estimates for debris disk studies at longer wavelengths were performed by Sibthorpe et al. (2013). As a first step, they convolve the Berta et al. (2011) number counts with Gaussians with various error estimates as a way of accounting for the Eddington bias. They present two calculations, one that calculates the probability of a single source producing the confusion and one that calculates the probability of one or more sources producing it. They also introduce a Monte Carlo style algorithm to calculate the probability of confusion. However, their algorithm considers the survey limiting flux density not just as a detection threshold, but also as the minimum galaxy flux in the model. For the 7'' model, at $S_{\text{lim}} = 6.39$ mJy, they predict a probability of 7.8%, which is close to the value given by our “point-sources” model. However, the methods of sky subtraction are not introduced in the paper, therefore we are unable to access the final results presented in it.

The cold disk candidate HIP 92043 is analyzed in Marshall et al. (2013). They also include a statistical argument whether the source can plausibly be a cold disk source in their section 4.1. Although they add a cold component to their model to fit at 160 μm , they describe their excess detection at this wavelength as marginal. Their statistical analysis is along the lines of that of Eiroa et al. (2013) and predict 1% of the sources having a contamination at the 12.9 mJy level. As a comparison, our CDF model predicts 2.1% of the sources having a contamination above the 12.9 mJy level for the “point-sources”, and 1.8% of them for the “PSF smoothed-sources” model at their assumed 11.3'' target aperture. Our higher values are due to the same effects as previously. They also cite the work of Sibthorpe et al. (2013), however, only consider their model where confusion with a single bright source is calculated. The MC models of Sibthorpe et al. (2013) show higher probabilities of confusion than their single source confusion analytic estimates.

8. SUMMARY

In this paper, we evaluate the hypothesis of a newly discovered class of *Herschel* cold debris disks (Eiroa et al. 2011, 2013; Krivov et al. 2013). We test whether the apparent temperature and flux distributions are instead consistent with confusion noise. Although this scenario has been considered by previous work, there are a few differences between our analyses:

- we simulate confusion noise using the full relevant range of background galaxy fluxes and allow for confusion from multiple sources,
- we account for the smoothing of the emissions by the PSF of the telescope,
- we develop an analysis method that accounts for the censorship of the data due to the limitations in signal to noise ratio in the DUNES 160 μm data.

We test the hypothesis that the distribution of cold debris disks is entirely due to confusion with background galaxies

(after rejecting cases with elevated noise from IR cirrus). We evaluate the hypothesis as a function of the target radius used to measure sources at 160 μm . We find that there is a greater-than-80% probability that the two distributions (confusion noise and the proposed cold debris disks) are indistinguishable, so long as the confusion beam is between 2 and 8'' in radius. This range of beam size includes all plausible values for the DUNES measurements. We conclude that the background confusion hypothesis is a viable alternative to the cold debris disk explanation for the 160 μm detections of these sources.

We thank Benjamin Weiner, Brandon Kelly, Eric Feigelson, and Ewan Cameron for inputs on the statistical analysis as well as the Astrostatistics and Astroinformatics Portal (ASAIP) hosted by Pennsylvania State University. Support for this work was provided by NASA through Contract Number 1255094 issued by JPL/Caltech.

REFERENCES

- Backman, D. E., Dasgupta, A., & Stencel, R. E. 1995, *ApJ*, 450, L35
 Bailey, V., Meshkat, T., Reiter, M., et al. 2014, *ApJ*, 780, L4
 Ballering, N. P., Rieke, G. H., Su, K. Y. L., & Montiel, E. 2013, *ApJ*, 775, 55
 Berta, S., et al. 2011, *A&A*, 532, A49
 Berta, S., et al. 2013, *A&A*, 551, A100
 Bracco, A., et al. 2011, *MNRAS*, 412, 1151
 Condon, J. J. 1974, *ApJ*, 188, 279
 Currie, T., Daemgen, S., Debes, J., et al. 2014, *ApJ*, 780, L30
 Dole, H., Lagache, G., & Puget, J.-L. 2003, *ApJ*, 585, 617
 Eiroa, C., et al. 2011, *A&A*, 536, L4
 Eiroa, C., et al. 2013, *A&A*, 555, A11
 Feigelson, E. D., & Nelson, P. I. 1985, *ApJ*, 293, 192
 Fernandez-Conde, N., Lagache, G., Puget, J.-L., & Dole, H. 2008, *A&A*, 481, 885
 Franceschini, A., Rodighiero, G., Vaccari, M., Berta, S., Marchetti, L., & Mainetti, G. 2010, *A&A*, 517, A74
 Gáspár, A., Psaltis, D., Rieke, G. H., & Özel, F. 2012, *ApJ*, 754, 74
 Grupponi, C., et al. 2013, *MNRAS*, 432, 23
 Hogg, D. W. 2001, *AJ*, 121, 1207
 Hogg, D. W., & Turner, E. L. 1998, *PASP*, 110, 727
 Kalas, P., et al. 2008, *Science*, 322, 1345
 Kaplan, E. L., & Meier, P. 1958, *Journal of the American Statistical Association*, 53, 457
 Kraus, A. L., Ireland, M. J., Cieza, L. A., et al. 2014, *ApJ*, 781, 20
 Krivov, A. V., Eiroa, C., Löhne, T., et al. 2013, *ApJ*, 772, 32
 Lagrange, A.-M., et al. 2010, *Science*, 329, 57
 Magnelli, B., et al. 2013, *A&A*, 553, A132
 Marois, C., Macintosh, B., Barman, T., Zuckerman, B., Song, I., Patience, J., Lafrenière, D., & Doyon, R. 2008, *Science*, 322, 1348
 Marshall, J. P., Krivov, A. V., del Burgo, C., et al. 2013, *A&A*, 557, A58
 Martin, P. G., et al. 2010, *A&A*, 518, L105
 Miville-Deschênes, M.-A., Lagache, G., Boulanger, F., & Puget, J.-L. 2007, *A&A*, 469, 595
 Morales, F. Y., Rieke, G. H., Werner, M. W., Bryden, G., Stapelfeldt, K. R., & Su, K. Y. L. 2011, *ApJ*, 730, L29
 Rameau, J., Chauvin, G., Lagrange, A.-M., et al. 2013, *ApJ*, 772, L15
 Roy, A., et al. 2010, *ApJ*, 708, 1611
 Rujopakarn, W., Rieke, G. H., Weiner, B. J., Pérez-González, P., Rex, M., Walth, G. L., & Kartaltepe, J. S. 2013, *ApJ*, 767, 73
 Scholz, F. W., & Stephens, M. A. 1987, *Journal of the American Statistical Association*, 82, 399
 Sibthorpe, B., Ivison, R. J., Massey, R. J., Roseboom, I. G., van der Werf, P. P., Matthews, B. C., & Greaves, J. S. 2013, *MNRAS*, 428, L6
 Symeonidis, M., et al. 2013, *MNRAS*, 431, 2317
 Veneziani, M., Piacentini, F., Noriega-Crespo, A., Carey, S., Paladini, R., & Paradis, D. 2013, *ApJ*, 772, 56
 Vitense, C., Krivov, A. V., Kobayashi, H., Löhne, T. 2012, *A&A*, 540, A30
 Yamamoto, S., & Mukai, T. 1998, *Earth, Planets, and Space*, 50, 531

